Enhanced energy recovery via separate hydrogen and methane production from two-stage anaerobic digestion of food waste with nanobubble water supplementation

Tingting Hou, Jiamin Zhao, Zhongfang Lei*, Kazuya Shimizu, Zhenya Zhang

Graduate School of Life and Environmental Sciences, University of Tsukuba, 1-1-1 Tennodai, Tsukuba, Ibaraki 305-8572, Japan

**Corresponding author. Email address:* lei.zhongfang.gu@u.tsukuba.ac.jp

Abstract

This study investigated the enhancement effect on two-stage anaerobic digestion (AD) of food waste (FW) for separate production of hydrogen and methane with N_2- and Air-nanobubble water (NBW) supplementation. In the first stage for hydrogen production, the maximum cumulative H_2 yield (27.31 ± 1.21 mL/g-VS) was obtained from FW supplemented with Air-NBW (FW+Air-NBW), increasing by 38% compared to the control (with deionized water (DW) addition). In the second stage for methane production, the cumulative CH_4 yield followed a descending order of FW+Air-NBW (373.63 ± 3.58 mL/g-VS) > FW+N_2-NBW (347.63 ± 7.05 mL/g-VS) > FW+DW (300.93 ± 3.24 mL/g-VS, control), increasing by 24% in FW+Air-NBW and 16% in FW+N_2-NBW compared to the control, respectively. Further investigations revealed that the positive effect of added N_2-NBW to the two-stage AD of FW was attributable to the enhanced hydrolysis of FW, while the addition of Air-NBW not only promoted the hydrolysis of FW with enhanced activities of four extracellular hydrolases at the end of hydrolysis/acidification stage, but also improved the methanogenesis indicated by enhanced activity of coenzyme

F_{420} at the end of methanogenesis stage. Results from this study suggest the potential application of NBW in the two-stage AD for efficient renewable energy recovery from FW.

Keywords: Food waste; Nanobubble water; Two-stage anaerobic digestion; Hydrogen; Methane

1. **Introduction**

Continuous growth of population and the scarcity of resources bring about the exhaustion of energy, thus the importunity and dependence on energy continues to reach record levels. “Turning waste into wealth” opens up a new path for sustainable utilization and management of wastes, which is increasingly attracting the attention from the society nowadays. As it is known, anaerobic digestion (AD) can convert organic wastes into renewable energy like H_2 and CH_4, which may relieve the pressure of energy scarcity and increase the diversity of fuel sources. From the viewpoint of environmental and economic aspects, bioconversion of organic wastes can reduce the risk of environmental pollution and disposal costs (Awasthi et al., 2018).

Municipal solid waste as the main source of organic wastes is estimated to be annually 2.3 billion tonnes by 2025, with food waste (FW) accounting for the largest proportion (≥ 50%) (Ahamed et al., 2016; Qin et al., 2019). According to the UN Food and Agriculture Organization (FAO), the roughly same quantities of food were dissipated in industrialized and less industrialized countries (670 and 630 million tonnes per annum), but FW is more problematic in industrialized countries, i.e. those countries with per capita FW by consumers between 95-115 kg per annum in Europe and North America as against 6-11 kg per annum in the low income Sub-Saharan

Africa and South/Southeast Asia regions (FAO, 2014). If not handled properly, one million tonnes of FW would cause 4.5 million tonnes of CO_2 emission from the landfill. In contrast, if being treated by AD, one million tonnes of FW could produce enough electricity to power 29,818 households (Kosseva, 2009). As a result, AD is considered as an appropriate option for the disposal of FW. However, due to the highly biodegradable components in FW, large amounts of volatile fatty acids (VFAs) produced quickly may result in a reduced pH to inhibit the activity of methanogens at the early stage of AD, which is claimed as the main reason for the failure of FW-AD reactors (Liu and Liao, 2019). Two-stage AD can separate the complicated AD process into two main stages, i.e. hydrolysis/acidification and methanogenesis, ensuring the optimal and different growth environment for the corresponding microbial groups. In the first stage, the complex organic compounds can be maximally degraded into short-chain VFAs under slightly acidic condition (pH = 5.0-6.0), from which hydrogen as a clean energy with high specific energy content (142 kJ/g) can be produced as an important intermediate in addition to VFAs (Silva et al., 2018; Yuan et al., 2019); in the second stage, the produced VFAs can be converted into methane by methanogens under relatively neutral condition (pH = 7.0-8.0) (Voelklein et al., 2016). Thus, two-stage AD is deemed to be promising to reduce organic loads and improve overall energy conversion efficiency besides the generation of the two high-calorie gases, i.e. H_2 and CH_4. As reported by Baldi et al. (2019), the biogas production and volatile solid (VS) degradation rate from two-stage AD of FW and activated sludge were increased by 26% and 9% in comparison to the single-stage AD, respectively.

However, the composition of FW is complex, rich in carbohydrates (41-62%), proteins (15-25%), and lipids (13-30%) (Boonpiyo et al., 2018). Although the high content of carbohydrates in FW can be easily converted, the high contents of proteins, lipids, and some recalcitrant cellulosic materials may greatly reduce the hydrolysis efficiency (Kim et al., 2019). On the other hand, the low hydrogen yield in the first stage might be the major limiting factor for the two-stage AD (Yuan et al., 2019). To enhance hydrolysis and biogas production, various pretreatment methods have been attempted to treat FW. For instance, Ding et al. (2017) applied hydrothermal pretreatment on FW, and obtained the maximum hydrogen and methane yields about 43.0 and 511.6 mL/g-VS under the optimum condition (140°C, 20 min), increasing by 24% and 32% when compared with the untreated FW, respectively. Acidic (pH = 2) and alkaline (pH = 11-12) pretreatments are also frequently adopted to FW due to their simple operations (Kim et al., 2014; Jang et al., 2015), from which hydrogen production can be largely improved while adversely impacted by operation mode. Although these pretreatments improve the hydrolysis of FW and thus enhance biogas production to some extent, the difficulty in maintenance of the operating conditions and the expensive chemicals addition greatly hinder their practical application.

Recently, nanobubble water (NBW) containing nano-scale bubbles (NBs) with diameter < 1000 nm has been applied for environmental remediation due to its unique characteristics (such as the long-term stable existence of NBs and the generation of hydroxyl radicals) and zero pollution (Azevedo et al., 2019; Hu and Xia, 2018; Li et al., 2014). It is worth mentioning that NBW addition has also been proven as an environmentally friendly method to enhance AD of organic solid wastes such as waste activated sludge and cellulosic materials (Wang et al., 2019; Yang et al., 2019; Wang et al., 2020a; Wang et al., 2020b). These previous works indicate that supplementation of various gas-NBW can enhance the hydrolysis of organic solids with enhanced methane production. Up to the present, however, no report is available about the effect of NBW on hydrogen production from AD, especially the two-stage AD process of high organic content wastes (like FW in this study).

In this study, N_2-NBW and Air-NBW were selected for the tests due to their different initial anaerobic (N_2-NBW) or micro-aerobic environment (Air-NBW) created after addition. Both hydrogen and methane production from the two-stage AD of FW were monitored. The underlying mechanisms of NBW addition to each stage were further explored for the first time by using the model substrates in the separate hydrolysis/acidogenesis and methanogenesis experiments. Finally, the enzyme activities with or without NBW addition were also evaluated to evidence the above mechanisms.

2. **Materials and methods**

2.1 FW, inoculum and NBW

FW was directly collected from the dormitory kitchen in University of Tsukuba, Japan, and the inoculum, anaerobically digested sludge was sampled from a wastewater treatment plant in Tsuchiura, Ibaraki Prefecture, Japan. The details of preparation and storage of FW and inoculum have been described previously (Hou et al., 2020). The physicochemical characteristics of FW and inoculum are shown in Table 1.

Table 1

The NBW, i.e. N_2-NBW or Air-NBW was prepared using the NBW generator (HACK FB11, Japan) under the optimal generation condition with NBs size of ~140 nm and the bubble particle concentration > 100 million particles/ml according to a previous work (Wang et al., 2019). Air used for Air-NBW generation was taken directly from the natural environment of the laboratory and the purity of N_2 used for N_2-NBW generation was ≥ 99.9995%.

2.2 Experimental set-up of the two-stage AD of FW system

2.2.1 Batch biochemical hydrogen potential (BHP) tests

The Schott Duran serum bottles with identical specification (250 mL in total volume with 150 mL of working volume) were used in both stages of experiments. In the BHP tests, each bottle was loaded with the same amount (20.0 g wet weight) of FW and 60 mL inoculum. After that, 70 mL of deionized water (DW), N_2-NBW, or Air-NBW was added to make the total working volume of each bottle to be 150 mL, in which the DW group was used as a blank control. In addition, the initial total VS in each bottle was 13.96 ± 0.49 g/L and the feed-to-microorganisms (F/M) ratio was about 6.5 (VS basis). As reported by Yuan et al. (2019), a high F/M ratio could inhibit the activity of methanogens in untreated inoculum, and a higher hydrogen yield could be achieved at a greater F/M ratio. More specifically, all the initial pH values were adjusted to 5.50 ± 0.10 using a 2 M HCl solution in the BHP tests, which is regarded as the optimal pH for the activity of enzyme hydrogenase and also could inhibit the activity of methanogens to avoid methane production (Liu et al., 2019; Micolucci et al., 2014).

2.2.2 Batch biochemical methane potential (BMP) tests

In the BMP tests, the remaining acidified slurries or mixtures from the BHP tests were used as substrates for the second stage to produce methane. 80 mL of acidified slurry and 50 mL of inoculum (with 4.5 of F/M ratio (VS basis) and 7.18 ± 0.40 g/L of initial total VS) were added into each bottle and then 20 mL of DW, N_2-NBW or Air-NBW was added to make the total working volume of each bottle to be 150 mL. In this stage, the initial pH value was adjusted to 7.50 ± 0.10 using a 2 M NaOH or HCl solution, which has been reported as the optimal pH for methanogens (Liu et al., 2019; Micolucci et al., 2014). Additionally, the inoculum was activated for about two weeks under mesophilic condition (38 ± 1℃) until no gas production and the TS and VS of inoculum were about 0.67% ± 0.01% and 0.42% ± 0.01% after activation, respectively.

Before starting the experiments, all the bottles were flushed with N_2 gas (purity ≥ 99.9995%) for 2 min for 3 times to ensure anaerobic conditions and then incubated in a temperature-controlled incubator (38 ± 1℃) for 68 h in the first-stage AD for hydrogen production and 24 d in the second-stage AD for methane production. In the BHP tests, the first gas sample was taken 8 h later, and then regularly collected over time every 12 h to detect the contents of H_2 and CO_2. In the BMP tests, the gas sample was regularly collected over time every 2 d to detect the contents of CH_4 and CO_2.

2.3 Effect of NBW addition on each stage in the two-stage AD by using the model substrates

The two-stage AD consists of two steps: hydrolysis/acidification and methanogenesis. The hydrolysis stage that can break down carbohydrates, proteins, and lipids into monosaccharides, amino acids, and long-chain fatty acids is crucial for complex organic compounds like FW (Dong et al., 2019). In this study, the effect of NBW addition on each stage in the two-stage AD system was investigated by using the model substrates (protein, glucose, and acetic acid (HAc)).

The experiments were carried out with 100 mL glass serum bottles. Firstly, for the hydrolysis process, 1500 mg/L of protein as the model substrate together with 25 mL of inoculum was loaded. Moreover, the total working volume was made up to 50 mL with 25 mL of DW, N_2-NBW, or Air-NBW, respectively. The concentration of protein in the filtrated supernatant from each bottle was daily monitored during the 8 days' hydrolysis to illustrate the effect of NBW addition. During the acidogenesis process, except the use of glucose (1500 mg/L) instead of protein as the model substrate, all the other operation conditions were the same as the hydrolysis step. During the examination, the concentration of glucose in the filtrated supernatant from each bottle was analyzed by sampling every 3 h for 12 h for to assess the effect of NBW addition on the acidogenesis step. Finally, HAc was used as the model substrate for the methanogenesis stage due to the fact that HAc was the main contributor to methane production according to the VFAs measurement in this study (section 3.1.2). A mixture with 90 mg of HAc (1500 mg/L) and 30 mL of inoculum was added into the designated bottles, then 30 mL of DW, N_2-NBW, or Air-NBW was added to make the total volume up to 60 mL. The biogas composition was analyzed every 2 days to calculate the cumulative methane yield during the 10 days' methanogenesis stage.

In all the above experiments prior to start, each bottle was firstly sealed with a rubber stopper and an resin crimp cap, and then flushed with high-purity N_2 gas (⩾ 99.9995%) for 1 min for 3 times to remove oxygen and finally placed in a temperature-controlled incubator (38 ± 1℃).

2.3 Microbial enzyme activities at each stage

To a great extent, the stability and efficiency of AD of organic wastes depend on the activity of microorganisms, and the main functional microorganisms in each stage are different in the two-stage AD process (Ma et al., 2019). Thus, the major microbial enzyme activities were evaluated in this study, aiming to provide insights into the effects of NBW addition on the two-stage AD of FW.

Four extracellular hydrolases, i.e. alkaline phosphatase (ALP), acid phosphatase (ACP), α-glucosidase, and protease (at the end of the first stage), and coenzyme F_{420} (at the end of the second stage) were measured. For their analysis, the activities of ALP, ACP, and α-glucosidase were measured according to Goel et al. (1998). 0.1% *p*-nitrophenyl phosphate disodium salt (pnpP), 0.1% pnpP, and 0.1%

p-nitrophenyl-α-D-glucopyranoside were used as substrates for the determination of ALP, ACP, and α-glucosidase, respectively. Besides, the activity of protease was analyzed according to the Folin-Phenol reagent method with 10 mg/mL of casein as the substrate (Dai et al., 2017; Ledoux and Lamy, 1986). Finally, coenzyme F_{420} was measured according to the method described by Delafontaine et al. (1979) and Dong et al. (2019).

In this study, the relative enzyme activity was calculated to evaluate the effect of NBW addition on microorganisms according to Eq. (1).

$$\text{Relative enzyme activity } (\%) = \frac{A_{NBW}}{A_{DW}} \times 100\% \quad (1)$$

where A_{NBW} and A_{DW} represent the absorbance at the same wavelength of the NBW added sample and DW added sample, respectively.

2.4 Other analytical methods and calculations

The determinations of total solid (TS) and VS of FW and inoculum were based on the standard methods (APHA, 2012). All liquid samples were filtered through 0.45 μm membrane filters before being analyzed and all the measurements were performed in triplicate. The concentrations of protein and glucose were determined by Lowry's method and Phenol-sulfuric acid method, respectively (Dubois et al., 1956; Lowry et al., 1951). Soluble total organic carbon (sTOC) was determined by a total carbon analyzer (TOC-VCSN with ASI-V autosampler, Shimadzu, Japan). pH value was determined with a semi-solid pH meter (Testo 206, Germany). According to the detailed description of Huang et al. (2016), the concentration of individual VFA, including the HAc, propionic acid (HPr), *iso*-butyric acid (*iso*-HBu), *n*-butyric acid (*n*-HBu), *iso*-valeric acid (*iso*-HVa), and *n*-valeric acid (*n*-HVa)), were determined by a gas chromatograph (GC-8A, Shimadzu, Japan) equipped with Unisole F-200 30/60 column and flame ionization detector.

For the gas samples, the volume of biogas production was measured using 50 and 20 mL of gas-tight syringes and normalized to standard temperature and pressure (25 °C, 1 atm). The contents of H_2, CH_4, and CO_2 in biogas were analyzed using a gas chromatograph (GC-8A, Shimadzu, Japan) after sampling 1 mL biogas produced and the volumes of hydrogen and methane were calculated according to Eq. (2).

$$V_{\mathrm{t}} = C_t \cdot V_{biogas,t} + V_{\mathrm{head}} \cdot \left(C_{\mathrm{t}} - C_{t\text{-}1}\right) \quad (2)$$

Additionally, the productions of hydrogen or methane during the interval between *t* and *t-1* were calculated based on VS in this study, according to Eq. (3).

$$Y_{\mathrm{t}} = \frac{V_{\mathrm{t}}}{\text{Total VS}} \quad (3)$$

where V_t (H_2 or CH_4) (mL) is the volume of hydrogen or methane produced during the interval between times *t* and *t-1*; C_t (%) and C_{t-1} (%) are the contents of hydrogen or methane at times *t* and *t-1*; $V_{biogas,t}$ (mL) is the volume of biogas produced at time *t*; V_{head} (mL) is the headspace volume of the bottle; Y_t (H_2 or CH_4, mL/g-VS) is the yield of hydrogen or methane based on VS during the interval between *t* and *t-1*.

In the BHP and BMP tests, the experimental data of cumulative hydrogen or methane yield in each stage was fitted to the modified Gompertz model as in Eq. (4).

$$H_{\mathrm{t}} \text{ or } M_t = P\, exp\{-exp[\frac{R_{max}}{P}(\lambda\text{-}t)]\} \quad (4)$$

where H_t or M_t (mL/g-VS) is the specific hydrogen or methane yield at a given time *t*; *P* (mL/g-VS) is the maximum hydrogen or methane production potential; R_{max} (mL/g-VS·h or mL/g-VS·d) is the maximum hydrogen or methane production rate; λ (h or d) is the lag time; *t* (h or d) is the experimental duration; and *e* =2.7183.

In this study, the energy recovery from the two-stage AD of FW with or without the NBW addition was calculated according to Eq. (5).

$$E_r = 12.78 \times Y_{H_2,\text{yield}} + 40.03 \times Y_{CH_4,yield} \quad (5)$$

where E_r (kJ/g-VS) is the energy recovery from the two-stage AD of FW; $Y_{H_2,\text{yield}}$(L/g-VS) is the hydrogen yield in the first stage; $Y_{CH_4,\text{yield}}$(L/g-VS) is the methane yield in the second stage. The heating value of H_2 (12.78 kJ/L) or CH_4 (40.03 kJ/L) under 1 atm and 25℃ was estimated according to the density and calorific value of H_2 or CH_4 gas, i.e., 0.09 kg/m^3 and 0.72 kg/m^3 or 142 kJ/g and 55.6 kJ/g, respectively (Silva et al., 2018).

2.5 Statistical analysis

All the experiments were carried out in duplicate and the sample was measured in triplicate. The data were processed by Microsoft Excel 2010 and expressed as the mean value ± standard deviation (SD). One-way analysis of variance (ANOVA) was also applied for statistical analysis and statistical significance was assumed at $p < 0.05$. Origin 9.0 (Origin Lab, trial version) was used to draw and analyze the fitting curve.

3. **Results and discussion**

3.1 Hydrogen production from the first stage of two-stage AD of FW

3.1.1 Hydrogen yield and kinetics analysis

The results of hourly H_2 production and cumulative H_2 yield in the BHP tests with the addition of DW or NBW (N_2-NBW and Air-NBW) are shown in Fig.1. It's important to mention that during the whole H_2 production process, no methane production was detected. The hourly H_2 productions from all the bottles were almost identical during the first 20 h ($p = 0.98 > 0.05$) and then increased to the peak values of 13.08 ± 0.06, 15.07 ± 0.46, and 16.10 ± 0.03 mL/g-VS·h at 32 h in FW+DW, FW+N_2-NBW, and FW+Air-NBW, respectively (Fig. 1 a). In addition, the hourly H2 productions from the NBW added reactors were also higher than that from the control with DW addition after reaching the peak values. These results indicate that addition of NBW can enhance H_2 production. Similarly, the cumulative H_2 yields from the NBW added reactors were greater than that from the DW added reactor. It is interesting to notice that the maximum cumulative H_2 yield (27.31 ± 1.21 mL/g-VS) was obtained in the Air-NBW added reactor, about 38% higher than that from the control (19.79 ± 0.07 mL/g-VS). Meanwhile, the cumulative H_2 yield (25.42 ± 0.37 mL/g-VS) from the N_2-NBW added reactor was 28% higher than that from the control. This enhancement by NBW addition may be due to the fact that NBs in the NBW will collapse when contacted with the organic matters in FW to generate OH· free radicals, which could oxidize and decompose the organic matter, thereby accelerating the hydrolysis of FW (Ghadimkhani et al., 2016; Takahashi et al., 2007). On the other hand, the uneven mass transfer of organic matters in FW is regarded as one of the main reasons for its low biogas production efficiency. A previous work by Hu and Xia (2018) indicates that micro-nanobubbles might promote mass transfer efficiency, resulting in enhanced utilization and conversion efficiency of organic substrates. In comparison, although N_2-NBW can ensure a strictly anaerobic environment, the cumulative H_2 yield was 10% lower than that from the Air-NBW added reactor. This implies that the introduction of trace amounts of air (or O_2) would increase rather than inhibit hydrogen production. This observation is consistent with that by Fu et al. (2020) who found that the maximum hydrogen yield of 24.3 mL/g VS was achieved at an oxygen loading of 5 mL/g-VS, about 70% higher than that without micro-aeration during the two-stage AD of corn straw. In this study, the micro-aerobic environment was realized by adding Air-NBW, which needs further in-depth investigations before being applied in practice.

<u>**Fig. 1**</u>

The relevant parameters of the first stage were obtained by fitting the BHP experimental data to the Modified Gompertz model (Table 2). The results show that the maximum P_{H2} (27.66 mL/g-VS) and $R_{H2, max}$ value (4.37 mL/g-VS·h) were obtained in the Air-NBW added reactor, which was consistent with the actual experimental results in the BHP tests. In addition, the lag time (λ) was reduced slightly, in the NBW added reactors (16.88-17.10 h) compared to the control (17.56 h). It indicates that although the addition of NBW resulted in some change of the original environment for the microorganisms, it didn't affect the start-up of the reactor.

Table 2

3.1.2 VFAs evolution in the first-stage AD

The individual VFA and the total VFAs concentrations at the end of BHP tests are shown in Fig. 2 a. In comparison to the control, the total VFAs concentration was detected higher under NBW addition, increasing about 9% and 10% in FW+N_2-NBW and FW+Air-NBW reactors, respectively. It is worth noting that HAc and HBu were the major VFAs during the hydrogen production stage, amounting to > 90% of the total VFAs concentration, in agreement with previous observations (Luo et al., 2010; Yuan et al., 2019).

In this study, the highest HAc production (2954.09 ± 48.34 mg/L) was detected in the FW+Air-NBW reactor, which is corresponding to its highest H_2 production. However, the HBu concentration followed a descending order of FW+N_2-NBW (1889.62 ± 0.45 mg/L) > FW+Air-NBW (1775.84 ± 61.51 mg/L) > FW+DW (1583.59 ± 2.12 mg/L). This means that the addition of Air-NBW is more conducive to HAc production, while the addition of N_2-NBW is beneficial for HBu production. The molar ratio of HBu to HAc (B/A ratio), as a proportional indicator of H_2 yields from per mole hexose (Ghimire et al., 2015), is plotted in Fig. 2 b. Only a slight improvement in B/A ratio was observed in the NBW added reactors, which was 0.40, 0.45, and 0.42 in the FW+DW, FW+N_2-NBW, and FW+Air-NBW reactors, respectively. This result indicates that the addition of NBW may not alter the metabolic pathway to product hydrogen, and the increase of hydrogen yield might be contributed by the improved hydrolysis as discussed later.

<u>Fig. 2</u>

3.2 Methane production from the second-stage of the two-stage AD of FW

3.2.1 Daily methane production and cumulative methane yield

The remaining hydrolyzed and acidified organic slurries or mixtures at the end of BHP tests were further used as the substrates for methane production in the subsequent BMP tests. The results of daily CH_4 production and cumulative CH_4 yield are presented in Fig. 3. Regarding the daily CH_4 production (Fig. 3 a), all the test conditions behaved almost same during the first 6 days and all the reactors reached the peak values on day 8. However, the FW+Air-NBW reactor achieved the highest peak value of 133.90 ± 0.56 mL/g-VS·d, in comparison to 87.22 ± 6.28 and 115.17 ± 0.20 mL/g-VS·d from the FW+DW and FW+N_2-NBW reactors, respectively, which is in agreement with the VFAs concentrations in the three reactors (Fig. 2 a). It has been claimed that a high VFAs concentration is beneficial for methane production (De Gioannis et al., 2017). The BMP tests lasted 24 d and the cumulative CH_4 yields from the NBW reactors were significantly higher than the control with DW addition (p =0.01 < 0.05, Fig. 3 b). Similarly, the cumulative CH_4 yield followed a descending order of FW+Air-NBW (373.63 ± 3.58 mL/g-VS) > FW+N_2-NBW (347.63 ± 7.05 mL/g-VS) > FW+DW (300.93 ± 3.24 mL/g-VS), increasing by 24% and 16% when compared with the FW+DW reactor, respectively. This observation clearly shows that the addition of NBW can positively effect both hydrogen and methane productions in the two-stage AD of FW, especially under Air-NBW addition. This result also proves once again that the micro-aerobic environment created by Air-NBW addition can promote rather than inhibit AD process. Similar phenomenon could be found in a previous study (Wang et al., 2020b), in which enhanced methane production from AD of cellulose was achieved when O_2-containing gas NBW was supplemented. At the end of methanogenesis, the final VS degradation rates in the FW+DW, FW+N_2-NBW, and FW+Air-NBW reactors were 65.97% ± 0.92%, 71.18% ± 0.04%, and 74.33% ± 0.21%, respectively, indicating that addition of NBW can improve VS decomposition thus enhance hydrogen and methane production from the two-stage AD of FW. The above results also suggest that NBW-based two-stage AD process can successfully improve energy recovery from the AD of FW with no chemicals addition and no secondary pollution.

Fig. 3

3.2.2 Kinetics involved in biomethane production

The methanogenesis stage was also described with the parameters of P, R_{max}, and λ by fitting the experimental data to the Modified Gompertz model as shown in Table 2. The maximum P_{CH4} (375.25 mL/g-VS) and $R_{CH4,max}$ (174.84 mL/g-VS·d) were also obtained in the Air-NBW added reactor, followed by the N_2-NBW added reactor (P_{CH4} = 346.58 mL/g-VS, $R_{CH4,max}$ = 133.90 mL/g-VS·d) and the control (P_{CH4} = 300.93 mL/g-VS, $R_{CH4,max}$ = 100.29 mL/g-VS·d). When compared to the control, a remarkable increase in $R_{CH4,max}$ by about 34% was obtained in the N_2-NBW added reactor, with an increase by 74% in the Air-NBW added reactor. This observation further confirms that addition of NBW is beneficial for methane production. In addition, the lag phase of methanogenesis was not significantly different among the three test conditions, about 4.02-4.44 d, but was much shorter than that of the one-stage AD (8.24 d) in a previous study by using the same FW (Hou et al., 2020). This might be attributable to the fact that much more available substrates were produced from the first stage of the two-stage AD (Fu et al., 2020).

3.3 Effect of NBW addition on the specific individual step involved in the two-stage AD by using the model substrates

In this study, the effects of NBW addition on the hydrolysis/acidogenesis and methanogenesis were explored by using the model substrates to better understand the effects of NBW addition on the two-stage AD and the results are shown in Fig 4. As shown in Figs. 4 a and b, the hydrolysis and acidogenesis steps were significantly enhanced with the addition of NBW, especially under Air-NBW addition(p = 0.02 and 0.01< 0.05). Fig. 4 a shows that the concentration of protein decreased by 1190.18 ± 36.07, 1397.56 ± 45.08, and 1433.62 ± 9.02 mg/L and the degradation rates of protein were 67%, 79%, and 83% in the FW+DW, FW+N_2-NBW, and FW+Air-NBW reactors, respectively. Similarly, the concentration of glucose decreased by 1098.54 ± 76.5, 1208.7 ± 39.78, and 1315.8 ± 0.00 mg/L and the degradation rates of glucose were 69%, 76%, and 83% in the FW+DW, FW+N_2-NBW, and FW+Air-NBW reactors, respectively (Fig. 4 b). The increase in degradation rates of these two model substrates further illustrates that the addition of NBW enhanced the hydrolysis and acidogenesis during the two-stage AD process. For the methanogenesis (Fig. 4 c), the cumulative methane yields were 94.89 ± 4.51, 100.93 ± 4.92, and 126.79 ± 5.12 mL/g-HAc in the FW+DW, FW+N_2-NBW, and FW+Air-NBW reactors, respectively. Most recently, Yang et al. (2019) found that the addition of N_2-NBW did not significantly enhance the methanogenesis of acetate, which agrees with the result from this study. The cumulative methane yield was only increased by 6% in the N_2-NBW added reactor when compared to the control (p = 0.85 > 0.05) in this study.

However, the methanogenesis was significantly enhanced with cumulative methane yield increased by 33% under Air-NBW addition ($p = 0.04 < 0.05$). Therefore, the positive effect of N_2-NBW addition on the two-stage AD of FW could attribute to the enhancement of hydrolysis/acidogenesis, while the addition of Air-NBW can not only promote the hydrolysis/acidogenesis of FW but also enhance the methanogenesis. This result was further confirmed by the enzyme activity as shown in section 3.4.

Fig. 4

3.4 Effects of NBW addition on the microbial enzyme activities at each stage

The relative activities of ALP, ACP, α-glucosidase, and protease at the end of the first stage (hydrolysis/acidification) and coenzyme F_{420} at the end of the second stage (methanogenesis) were determined and calculated to provide insights into the effects of NBW on microorganisms in the two-stage AD of FW. Clearly, the activities of four extracellular hydrolases under NBW addition were higher than those in the control (Fig. 5 a). In particular, the addition of Air-NBW achieved the highest activities of ALP, ACP, α-glucosidase, and protease, increasing by 29%, 47%, 14%, and 8% in comparison to the control, respectively. It has been reported that the phosphatases, including ALP and ACP, can catalyze the hydrolysis of organic phosphate esters and protease is capable of hydrolyzing soluble proteins into amino acids (Mu and Chen, 2011; Wan et al., 2020). In addition, the activity of α-glucosidase in the FW+N_2-NBW reactor increased by 23% compared with the control. The α-glucosidase is considered as a crucial enzyme for the conversion of disaccharides and oligosaccharides into monosaccharides (Ni et al., 2020). The increase of bioactivity in these hydrolases verified that addition of NBW could enhance the hydrolysis of FW under the test first-stage conditions.

As it is known, coenzyme F_{420} plays a critical role in the process of methanogenesis, which represents the conversion activity of the electron donor-driven by redox proton translocation in the methanogenic archaea (Mu and Chen, 2011). Fig. 5 b shows that the relative activity of F_{420} increased by 4% and 34% in the FW+N_2-NBW and FW+Air-NBW reactors in comparison to the control, respectively. Clearly, the addition of Air-NBW has a significantly positive effect on the activity of coenzyme F_{420}, resulting in improved methane production. This observation further confirms that the improvement on hydrogen and methane production from the two-stage AD of FW through Air-NBW supplementation may involve in enhanced microbial activities in both stages, i.e., hydrolysis/acidification and methanogenesis.

<u>Fig. 5</u>

As seen from the above results, Air-NBW is more suitable than N_2-NBW for the two-stage AD of FW to produce hydrogen and methane sequentially due to the following two reasons. Firstly, the air is preferable and free everywhere, which is easier to obtain than nitrogen. Thus, the manufacturing of Air-NBW can reduce cost and operation difficulty. Secondly, the addition of Air-NBW showed superior effectiveness than that of N_2-NBW in the test two-stage AD of FW either in terms of hydrogen production or methane production.

3.5 Energy recovery from the two-stage AD of FW with or without NBW addition

The energy recovery from H_2 and CH_4 in the two-stage AD of FW with or without NBW addition was analyzed as shown in Table 3. It is worth noting that the two-stage AD of FW achieved much higher energy recovery (12.30 kJ/g-VS in FW+DW) than one-stage AD using the same FW (9.68 kJ/g-VS) (Hou et al., 2020). This observation to some extent is in agreement with a previous work by Yuan et al. (2019) who reported 10% higher energy yield obtained in the two-stage AD of FW than the one-stage AD of FW. Owing to the addition of Air-NBW, the increment in energy recovery from the two-stage AD of FW is about 62% than the one-stage AD of FW. As pointed out by Fu et al. (2020), the first stage of two-stage AD can be regarded as biological pretreatment of high organic content wastes (such as FW in this study), in which hydrogen energy recovery and substrates pretreatment are realized simultaneously. In this study, the highest total energy recovery was obtained from the FW+Air-NBW reactor (15.31 ± 0.16 kJ/g-VS), increasing by 24% when compared to the FW+DW reactor.

Table 3

When considering the electricity consumption involved in manufacturing of NBW, the economic assessment is also necessary. In this study, Air-NBW addition was used as an example. The generation capacity of the NBW generator is 12-22 L/min (the median generation capacity (17 L/min) was used for calculation) at a power consumption of 0.75 kW·h. When 1 tonne of FW is treated, the required 4500 L of Air-NBW will consume 3.31kWh of electricity. The comparative economic assessment results between the FW+DW reactor and FW+Air-NBW reactor are shown in Table 4. The increase in generated electricity from the FW+Air-NBW reactor is about 23% when compared to the FW+DW reactor. When taking the more TS and VS reductions into consideration, supplementation of Air-NBW can be considered as an environmentally friendly technology for more renewable energy recovery from the two-stage AD of FW.

Table 4

4. Conclusions

The addition of NBW can achieve higher H_2 and CH_4 yields from the two-stage AD of FW than the control, especially under Air-NBW addition which increased H_2 yield by 38% and CH_4 yield by 24%. The relative activities of hydrolases increased by 8-47% in the first stage, and the activity of coenzyme F_{420} was significantly enhanced by 34% in the second stage with addition of Air-NBW. Therefore, the developed two-stage AD of FW with Air-NBW supplementation can enhance hydrogen and methane production simultaneously, greatly increasing (23%) the energy recovery from the whole AD system. This two-stage AD process is a promising and environmentally friendly approach, targeting the maximization of renewable energy recovery from FW.

Acknowledgements

The first author appreciated the financial support from the China Scholarship Council (CSC.201806400011) for her study in University of Tsukuba, Japan.

References

Ahamed, A., Yin, K., Ng, B.J.H., Ren, F., Chang, V.W.C., Wang, J.Y., 2016. Life cycle assessment of the present and proposed food waste management technologies from environmental and economic impact perspectives. J. Clean. Prod. 131, 607-614.

APHA, 2012. Standard Methods for the Examination of Water and Wastewater, 22nd edition. American Public Health Association/American Water Work Association/Water Environment Federation, Washington D.C., USA.

Awasthi, S.K., Joshi, R., Dhar, H., Verma, S., Awasthi, M.K., Varjani, S., Sarsaiya, S., Zhang, Z., Kumar, S., 2018. Improving methane yield and quality via co-digestion of cow dung mixed with food waste. Bioresour. Technol. 251, 259-263.

Azevedo, A., Oliveira, H., Rubio, J., 2019. Bulk nanobubbles in the mineral and environmental areas: Updating research and applications. Adv. Colloid Interfac.

271, 101992.
Baldi, F., Pecorini, I., Iannelli, R., 2019. Comparison of single-stage and two-stage anaerobic co-digestion of food waste and activated sludge for hydrogen and methane production. Renew. Energ. 143, 1755-1765.
Boonpiyo, S., Sittijunda, S., Reungsang, A., 2018. Co-digestion of napier grass with food waste and napier silage with food waste for methane production. Energies 11(11), 1-13.
Dai, X., Hu, C., Zhang, D., Dai, L., Duan, N., 2017. Impact of a high ammonia-ammonium-pH system on methane-producing archaea and sulfate-reducing bacteria in mesophilic anaerobic digestion. Bioresour. Technol. 245, 598-605.
De Gioannis, G., Muntoni, A., Polettini, A., Pomi, R., Spiga, D., 2017. Energy recovery from one- and two-stage anaerobic digestion of food waste. Waste Manage. 68, 595-602.
Delafontaine, M.J., Naveau, H.P., Nyns, E.J., 1979. Fluorimetric monitoring of methanogenesis in anaerobic digestors. Biotechnol. Lett. 1, 71-74.
Ding, L., Cheng, J., Qiao, D., Yue, L., Li, Y., Zhou, J., Cen, K., 2017. Investigating hydrothermal pretreatment of food waste for two-stage fermentative hydrogen and methane co-production. Bioresour. Technol. 241, 491-499.
Dong, B., Xia, Z., Sun, J., Dai, X., Chen, X., Ni, B., 2019. The inhibitory impacts of nano-graphene oxide on methane production from waste activated sludge in anaerobic digestion. Sci. Total Environ. 646, 1376-1384.
Dubois, M., Gilles, K.A., Hamilton, J.K., Revers, P.A., Smith, F., 1956. Colorimetric method for determination of sugars. Anal. Chem. 28, 350-356.
FAO (Food and Agriculture Organization), 2014. Reduction of food losses and waste in

Europe and Central Asia for improved food security and agrifood chain efficiency. <http://www.fao.org/3/a-au844e.pdf>.

Fu, S., Liu, R., Sun, W., Zhu, R., Zou, H., Zheng, Y., Wang, Z., 2020. Enhancing energy recovery from corn straw via two-stage anaerobic digestion with stepwise microaerobic hydrogen fermentation and methanogenesis. J. Clean. Prod. 247, 119651.

Ghadimkhani, A., Zhang, W., Marhaba, T., 2016. Ceramic membrane defouling (cleaning) by air nano bubbles. Chemosphere 146, 379-384.

Ghimire, A., Frunzo, L., Pirozzi, F., Trably, E., Escudie, R., Lens, P.N.L., Esposito, G., 2015. A review on dark fermentative biohydrogen production from organic biomass: Process parameters and use of by-products. Appl. Energ. 144, 73-95.

Goel, R., Mino, T., Satoh, H., Matsuo, T., 1998. Enzyme activities under anaerobic and aerobic conditions in activated sludge sequencing batch reactor. Water Res. 32(7), 2081-2088.

Hou, T., Zhao, J., Lei, Z., Shimizu, K., Zhang, Z., 2020. Synergistic effects of rice straw and rice bran on enhanced methane production and process stability of anaerobic digestion of food waste. Bioresour. Technol. 314, 123775.

Hu, L., Xia, Z., 2018. Application of ozone micro-nano-bubbles to groundwater remediation. J. Hazard. Mater. 342, 446-453.

Huang, W., Huang, W., Yuan, T., Zhao, Z., Cai, W., Zhang, Z., Lei, Z., Feng, C., 2016. Volatile fatty acids (VFAs) production from swine manure through short-term dry anaerobic digestion and its separation from nitrogen and phosphorus resources in the digestate. Water Res. 90, 344-353.

Jang, S., Kim, D., Yun, Y., Lee, M., Moon, C., Kang, W., Kwak, S., Kim, M., 2015. Hydrogen fermentation of food waste by alkali-shock pretreatment: Microbial community analysis and limitation of continuous operation. Bioresour. Technol. 186, 215-222.

Kim, J., Baek, G., Kim, J., Lee, C., 2019. Energy production from different organic wastes by anaerobic co-digestion: Maximizing methane yield versus maximizing synergistic effect. Renew. Energ. 136, 683-690.

Kim, D., Jang, S., Yun, Y., Lee, M., Moon, C., Kang, W., Kwak, S., Kim, M., 2014. Effect of acid-pretreatment on hydrogen fermentation of food waste: Microbial community analysis by next generation sequencing. Int. J. Hydrogen Energ. 39(29), 16302-16309.

Kosseva, M.R., 2009. Processing of food wastes. Food Nutr. Res. 58, 57-136.

Ledoux, M., Lamy, F., 1986. Determination of proteins and sulfobetaine with the Folin-Phenol. Anal. Biochem. 157, 28-31.

Li, H., Hu, L., Song, D., Lin, F., 2014. Characteristics of micro-nano bubbles and potential application in groundwater bioremediation. Water Environ. Res. 86(9), 844-851.

Liu, W., Liao, B., 2019. Anaerobic co-digestion of vegetable and fruit market waste in LBR + CSTR two-stage process for waste reduction and biogas production. Appl. Biochem. Biotech. 188(1), 185-193.

Liu, X., Li, R., Ji, M., 2019. Effects of two-stage operation on stability and efficiency in co-digestion of food waste and waste activated sludge. Energies 12(14), 2748.

Lowry, O.H.N.G., Rosebrough, N.J.J., Farr, A.L., Randall, R.J.R., 1951. Protein measurement with folin fenol reagent. J. Biol. Chem. 193, 265-275.

Luo, G., Xie, L., Zou, Z., Zhou, Q., Wang, J., 2010. Fermentative hydrogen production from cassava stillage by mixed anaerobic microflora: Effects of temperature and pH. Appl. Energ. 87(12), 3710-3717.

Ma, S., Ma, H., Hu, H., Ren, H., 2019. Effect of mixing intensity on hydrolysis and acidification of sewage sludge in two-stage anaerobic digestion: Characteristics of dissolved organic matter and the key microorganisms. Water Res. 148, 359-367.

Micolucci, F., Gottardo, M., Bolzonella, D., Pavan, P., 2014. Automatic process control for stable bio-hythane production in two-phase thermophilic anaerobic digestion of food waste. Int. J. Hydrogen Energ. 39(31), 17563-17572.

Mu, H., Chen, Y., 2011. Long-term effect of ZnO nanoparticles on waste activated sludge anaerobic digestion. Water Res. 45(17), 5612-5620.

Ni, M., Hu, X., Gong, D., Zhang, G., 2020. Inhibitory mechanism of vitexin on α-glucosidase and its synergy with acarbose. Food Hydrocoll. 105, 105824.

Qin, Y., Li, L., Wu, J., Xiao, B., Hojo, T., Kubota, K., Cheng, J., Li, Y., 2019. Co-production of biohydrogen and biomethane from food waste and paper waste via recirculated two-phase anaerobic digestion process: Bioenergy yields and metabolic distribution. Bioresour. Technol. 276, 325-334.

Silva, F.M.S., Mahler, C.F., Oliveira, L.B., Bassin, J.P., 2018. Hydrogen and methane production in a two-stage anaerobic digestion system by co-digestion of food waste, sewage sludge and glycerol. Waste Manage. 76, 339-349.

Takahashi, M., Chiba, K., Li, P., 2007. Free-radical generation from collapsing microbubbles in the absence of a dynamic stimulus. J. Phys. Chem. B 111(6), 1343-7.

Voelklein, M.A., Jacob, A., O Shea, R., Murphy, J.D., 2016. Assessment of increasing loading rate on two-stage digestion of food waste. Bioresour. Technol. 202,172-180.

Wan, W., Wang, Y., Tan, J., Qin, Y., Zuo, W., Wu, H., He, H., He, D., 2020. Alkaline phosphatase-harboring bacterial community and multiple enzyme activity contribute to phosphorus transformation during vegetable waste and chicken manure composting. Bioresour. Technol. 297,122406.

Wang, D., Yang, X., Tian, C., Lei, Z., Kobayashi, N., Kobayashi, M., Adachi, Y., Shimizu, K., Zhang, Z., 2019. Characteristics of ultra-fine bubble water and its trials on enhanced methane production from waste activated sludge. Bioresour. Technol. 273, 63-69.

Wang, X., Yuan, T., Guo, Z., Han, H., Lei, Z., Shimizu, K., Zhang, Z., Lee, D.-J., 2020a. Enhanced hydrolysis and acidification of cellulose at high loading for methane production via anaerobic digestion supplemented with high mobility nanobubble water. Bioresour. Technol. 297, 122499.

Wang, X., Yuan, T., Lei, Z., Kobayashi, M., Adachi, Y., Shimizu, K., Lee, D.-J., Zhang, Z., 2020b. Supplementation of O_2-containing gas nanobubble water to enhance methane production from anaerobic digestion of cellulose. Chem. Eng. J. 398, 125652.

Yang, X., Nie, J., Wang, D., Zhao, Z., Kobayashi, M., Adachi, Y., Shimizu, K., Lei, Z., Zhang, Z., 2019. Enhanced hydrolysis of waste activated sludge for methane production via anaerobic digestion under N_2-nanobubble water addition. Sci. Total Environ. 693, 133524.

Yuan, T., Bian, S., Ko, J.H., Wu, H., Xu, Q., 2019. Enhancement of hydrogen production using untreated inoculum in two-stage food waste digestion. Bioresour. Technol. 282, 189-196.

Table 1

Physicochemical characteristics of the food waste and inoculum used in this study

Parameter	Food waste	Inoculum
Total solids (TS, %)[a]	13.08 ± 0.12	0.70 ± 0.01
Volatile solid (VS, %)[a]	8.93 ± 0.18	0.45 ± 0.03
Total volatile fatty acids (VFAs, mg/L)	5287.74 ± 67.57	9.77 ± 1.70
Soluble total organic carbon (sTOC, mg/L)	10191.74 ± 21.63	171.61 ± 0.22

[a] Wet weight basis.

Table 2

Parameters estimated by fitting the experimental data from the first-stage and second-stage AD tests to the Modified Gompertz model

Stage/Reactors	Parameters in the modified Gompertz model			
The first-stage AD of FW				
	P_{H2} (mL/g-VS)	$R_{H2,max}$ (mL/g-VS·h)	λ (h)	R^2
FW+DW	19.84 ± 0.05	3.87 ± 0.08	17.56 ± 0.08	0.9999
FW+N_2-NBW	24.52 ± 0.15	4.32 ± 0.14	16.88 ± 0.22	0.9996
FW+Air-NBW	27.66 ± 0.29	4.37 ± 0.22	17.10 ± 0.41	0.9990
The second-stage AD of FW				
	P_{CH4} (mL/g-VS)	$R_{CH4,max}$ (mL/g-VS·d)	λ (d)	R^2
FW+DW	300.93 ± 2.78	100.29 ± 4.10	4.02 ± 0.17	0.9981
FW+N_2-NBW	346.58 ± 3.49	133.90 ± 6.77	4.05 ± 0.19	0.9974
FW+Air-NBW	375.25 ± 3.01	174.84 ± 8.33	4.44 ± 0.15	0.9981

Table 3

Energy recovery from the two-stage AD of FW with or without NBW addition

Reactors	Energy recovery (kJ/g-VS)		
	H_2 production in the first stage	CH_4 production in the second stage	Two-stage AD
FW+DW	0.25 ± 0.00	12.05 ± 0.13	12.30 ± 0.13
FW+N_2-NBW	0.32 ± 0.00	13.92 ± 0.28	14.24 ± 0.28
FW+Air-NBW	0.35 ± 0.02	14.96 ± 0.14	15.31 ± 0.16

Table 4

Comparative results of economic assessment between the FW+DW reactor and FW+Air-NBW reactor when treating 1 tonne of FW

Reactors	H_2 yield (L)	Heating value of H_2 (kJ)	CH_4 yield (L)	Heating value of CH_4 (kJ)	Total heating value (kJ)	Generated electricity (kWh)
FW+DW	1,767	22,582	26,873	1,075,726	1,098,308	305.09
FW+Air-NBW	2,439	31,170	33,365	1,335,601	1,366,771	376.35

The unit conversion from kJ to kWh is 1/3600.

Figure captions

Fig. 1. Time courses of daily H_2 production (a) and cumulative H_2 yield (b) under DW and NBW (N_2-NBW and Air-NBW) addition. DW: deionized water, NBW: nanobubble water.

Fig. 2. The individual VFA and total VFAs concentrations (a) and the molar HBu/HAc (B/A) ratio and H_2 yield (b) at the end of the first stage under DW and NBW (N_2-NBW and Air-NBW) addition. VFA: volatile fatty acid, DW: deionized water, NBW: nanobubble water.

Fig. 3. Time courses of daily CH_4 production (a) and cumulative CH_4 yield (b) under DW and NBW (N_2-NBW and Air-NBW) addition. DW: deionized water, NBW: nanobubble water.

Fig. 4. Effects of NBW (N_2-NBW and Air-NBW) addition on the specific individual step involved in two-stage anaerobic digestion by using the model substrates: (a) variation of protein concentration during hydrolysis step; (b) variation of glucose concentration during acidogenesis step; and (c) cumulative methane yield from HAc during methanogenesis. NBW: nanobubble water.

Fig. 5. Effects of NBW (N_2-NBW and Air-NBW) addition on the relative activity of ALP, ACP, protease, α-glucosidase, and protease at the end of the first stage (hydrolysis/acidification, a), and the relative activity of coenzyme F_{420} at the end of the second stage (methanogenesis, b). NBW: nanobubble water, ALP: alkaline phosphatase, ACP: alkaline phosphatase.

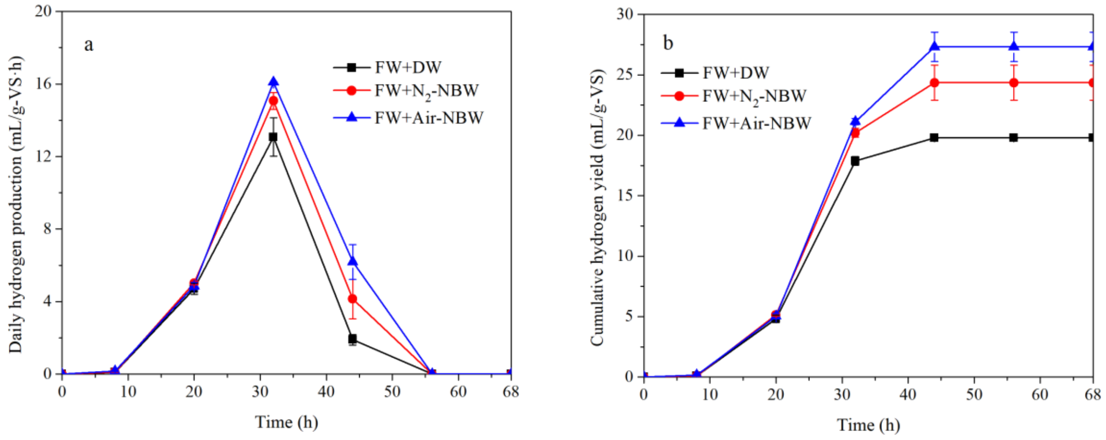
a
FW+DW
FW+N2-NBW
FW+Air-NBW
Daily hydrogen production (mL/g-VS·h)
Time (h)
b
Cumulative hydrogen yield (mL/g-VS)

Figure 1

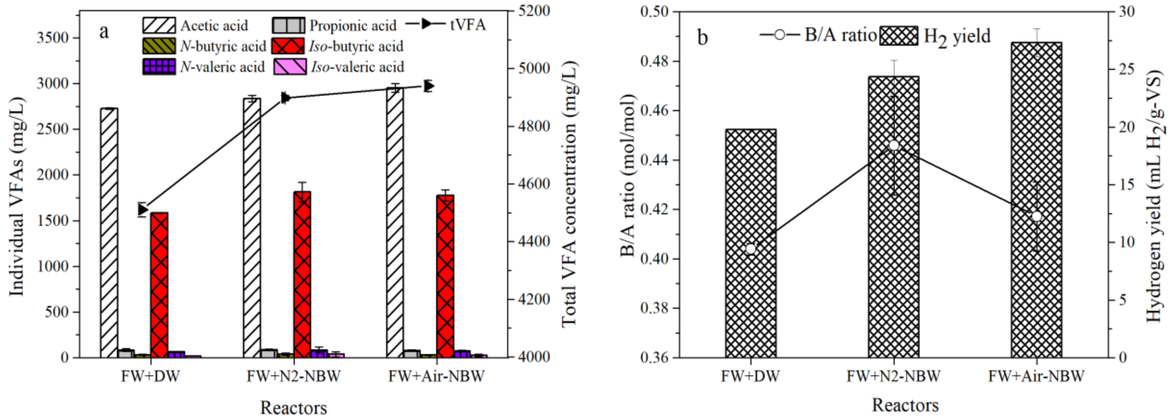
a
Acetic acid
Propionic acid
tVFA
N-butyric acid
Iso-butyric acid
N-valeric acid
Iso-valeric acid
Individual VFAs (mg/L)
Total VFA concentration (mg/L)
FW+DW
FW+N2-NBW
FW+Air-NBW
Reactors
b
B/A ratio
H2 yield
B/A ratio (mol/mol)
Hydrogen yield (mL H2/g-VS)
FW+DW
FW+N2-NBW
FW+Air-NBW
Reactors

Figure 2

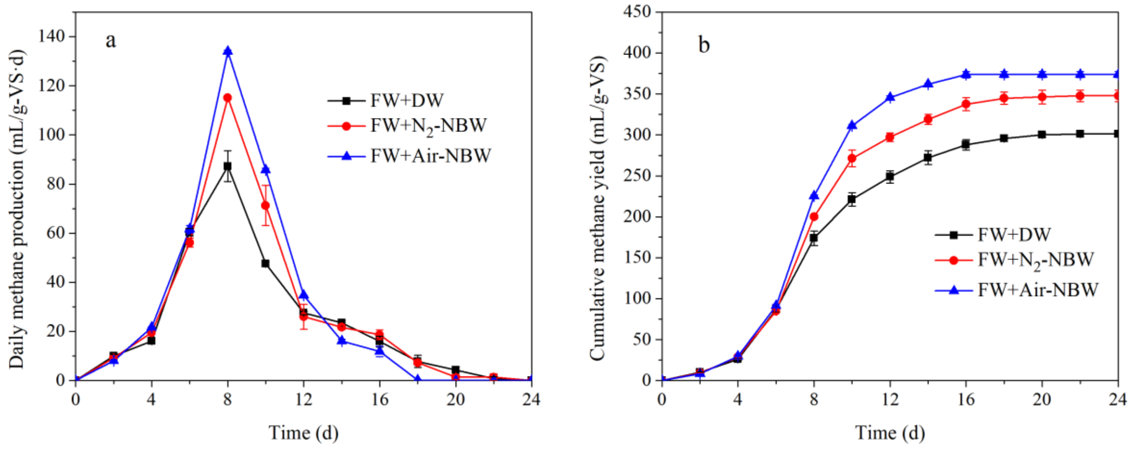
a
Daily methane production (mL/g-VS·d)
Time (d)
FW+DW
FW+N$_2$-NBW
FW+Air-NBW
b
Cumulative methane yield (mL/g-VS)
Time (d)
FW+DW
FW+N$_2$-NBW
FW+Air-NBW

Figure 3

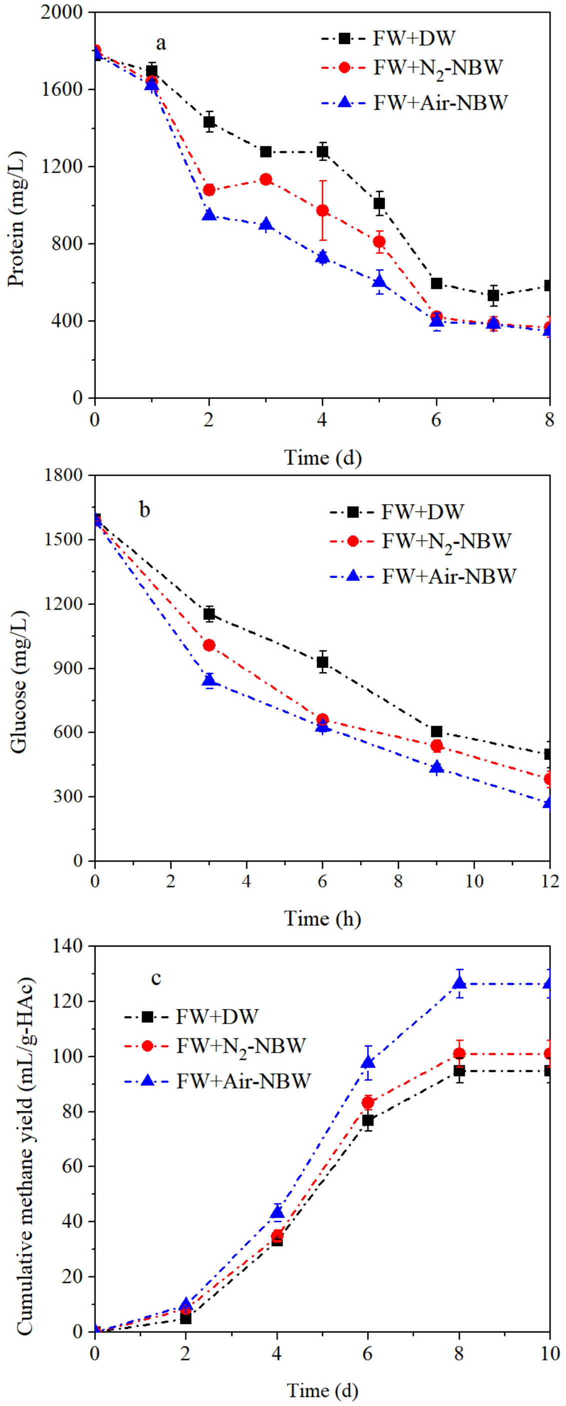
a
FW+DW
FW+N2-NBW
FW+Air-NBW
Protein (mg/L)
Time (d)
b
FW+DW
FW+N2-NBW
FW+Air-NBW
Glucose (mg/L)
Time (h)
c
FW+DW
FW+N2-NBW
FW+Air-NBW
Cumulative methane yield (mL/g-HAc)
Time (d)

Figure 4

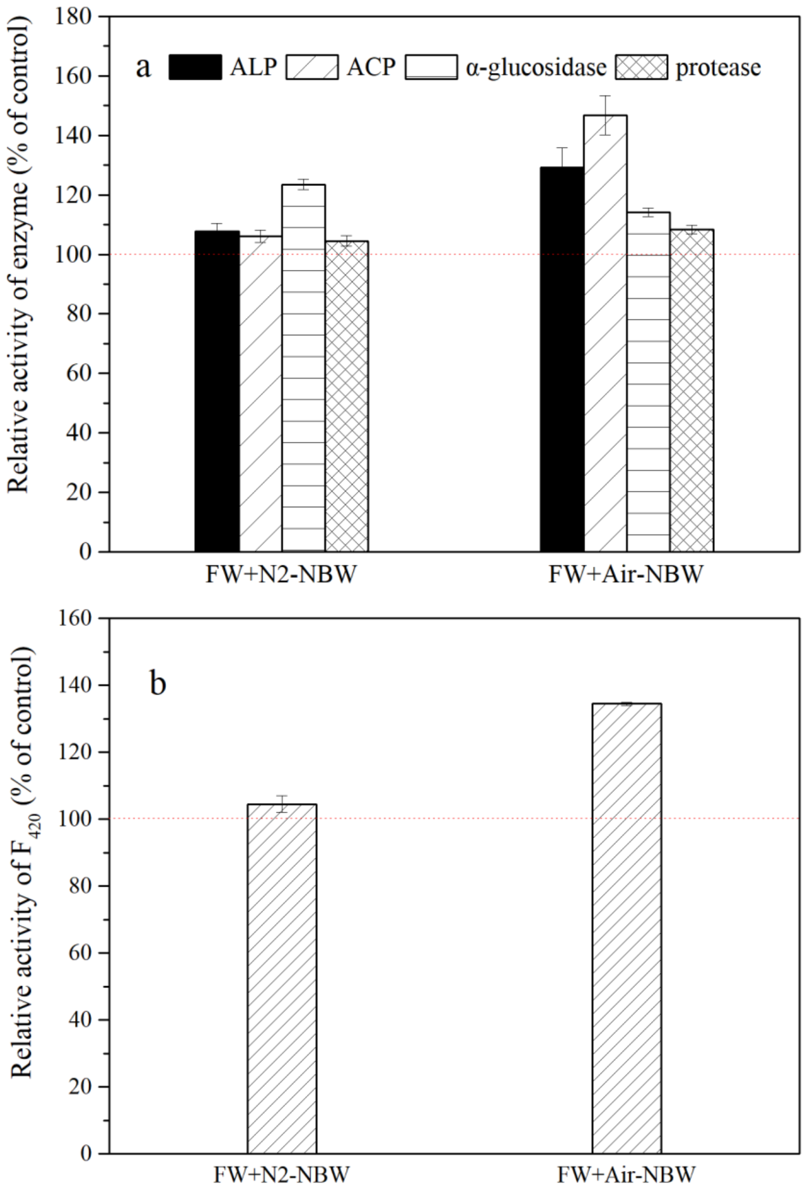

723

724 **Figure 5**

725